

Organic & Biomolecular Chemistry

Accepted Manuscript



This is an *Accepted Manuscript*, which has been through the Royal Society of Chemistry peer review process and has been accepted for publication.

Accepted Manuscripts are published online shortly after acceptance, before technical editing, formatting and proof reading. Using this free service, authors can make their results available to the community, in citable form, before we publish the edited article. We will replace this *Accepted Manuscript* with the edited and formatted *Advance Article* as soon as it is available.

You can find more information about *Accepted Manuscripts* in the [Information for Authors](#).

Please note that technical editing may introduce minor changes to the text and/or graphics, which may alter content. The journal's standard [Terms & Conditions](#) and the [Ethical guidelines](#) still apply. In no event shall the Royal Society of Chemistry be held responsible for any errors or omissions in this *Accepted Manuscript* or any consequences arising from the use of any information it contains.

COMMUNICATION

Combining an Hsp70 inhibitor with either an N- or C-terminal Hsp90 inhibitor produces mechanistically distinct phenotypes

Cite this: DOI: 10.1039/x0xx00000x

Received 00th January 2012,
Accepted 00th January 2012

Y. Wang, and S. R. McAlpine*

DOI: 10.1039/x0xx00000x

www.rsc.org/

Blocking the function of both heat shock protein 90 and 70 (Hsp90 and Hsp70) simultaneously limits these chaperones' cytoprotective effects on cancer cells. The unique phenotype associated with modulating Hsp90's C-terminus, when used in combination with Hsp70 inhibitors, produces a synergistic and highly relevant dual chemotherapy regimen.

Molecular chaperones heat shock protein 90 (Hsp90) and heat shock protein 70 (Hsp70) play critical roles in cancer cell growth as they fold and stabilize many proteins that are utilized in oncogenic pathways.¹⁻⁴ Numerous Hsp90 inhibitors have been utilized in over 50 clinical trials (clinicaltrials.gov database) targeting cancer, where all act via the same mechanism: they inhibit ATP from binding to Hsp90 (termed "classical inhibitors"). These classical inhibitors have had disappointing results, and most are now being utilized in dual therapies involving already approved cancer drugs (e.g. cisplatin and paclitaxel) (clinicaltrials.gov database). One reason behind their failure as single-treatment drug is that these classical Hsp90 inhibitors induce a cytoprotective response that is referred to as a heat shock response (HSR).⁵ This HSR generates high levels of Hsp70, Hsp40, and Hsp27 proteins, where these heat shock proteins (HSPs) support rapid cell division, maintain oncogenic cellular activity, and resist apoptosis that is triggered by Hsp90 inhibitors.⁶ Thus, the Hsp90 inhibitor-induced HSR is highly problematic as it protects the cells that are being targeted for apoptosis. Utilizing a combination of Hsp90 and Hsp70 inhibitors is an approach that may neutralize the HSR.

Hsp70 inhibitors have not yet been approved by the FDA, however combination therapy involving Hsp70 and Hsp90 inhibitors is already at early stages of development. Specifically, combination therapies using classical inhibitors (ie molecules that target the ATP binding site of Hsp70 and Hsp90 respectively) have proven effective in both *in vitro* and *in vivo* preclinical studies.⁷⁻¹⁰ However, since these studies utilize classical Hsp90 inhibitors they up-regulate Hsp70, while then concurrently inhibiting Hsp70 using a second molecule. There are several new classes of Hsp90 inhibitors that do not induce a HSR in cancer cells, nor do they produce large increases in the expression of Hsp70, Hsp40, or Hsp27 proteins.¹¹⁻¹⁴

The elevated protein level of Hsp70 is only seen with the molecules that disrupt the ATP-Hsp90 interaction, but not with those that block the access to the C-terminus of Hsp90, like SM122 (Fig. 1a).^{11, 12, 15} SM122 induces a distinct phenotype in cancer cells compared to treatments with classical Hsp90 inhibitors.¹⁵ Furthermore, using a C-terminal Hsp90 modulator such as SM122 in combination with a classical Hsp70 inhibitor (e.g. VER, Fig. 1a) produces strong synergistic effects in killing multiple cancer cell types.¹⁶ Treating cancer cells with SM122/VER produces severe damage in both Hsp90- and Hsp70-dependent protein folding systems, increases cell cycle disorder, and accelerates apoptosis.¹⁶ The synergistic behavior of SM122/VER triggers apoptotic cancer cell death more effectively than treatment with the classical inhibitors 17-AAG/VER.¹⁶ Given that SM122 does not induce the HSR but 17-AAG does^{11-13, 15, 17-20} we hypothesized that SM122/VER had distinct impacts on the HSR pathway making them more effective than 17-AAG/VER.

Herein we compare how treating cancer cells with either a combination of 17-AAG/VER or SM122/VER impacted the HSR induction mechanism. We assessed multiple steps in the combination therapy including their impact on (i) the mRNA transcription of HSPs (Hsp72 and Hsc70), (ii) the translation process, (iii) the HSPs' protein expression levels, and (iv) clients and co-chaperones (Fig. 1b). We reported that in HCT116 human colon cancer cells, the GI₅₀ of VER, 17-AAG, and SM122 were 22 μM, 50 nM, and 8 μM respectively.^{15, 16} In earlier studies that focused on cytotoxicity and protein folding we optimized the drug-ratios of 17-AAG/VER (3 : 1000) and SM122/VER (1 : 5) in HCT116 cells, and used 150 nM of 17-AAG or 10 μM of SM122 in combination with 50 μM of VER.¹⁶ Thus in this study we used HCT116 cell line and the synergistic drug combinations 17-AAG/VER = 150 nM/50 μM, SM122/VER = 10 μM/50 μM.

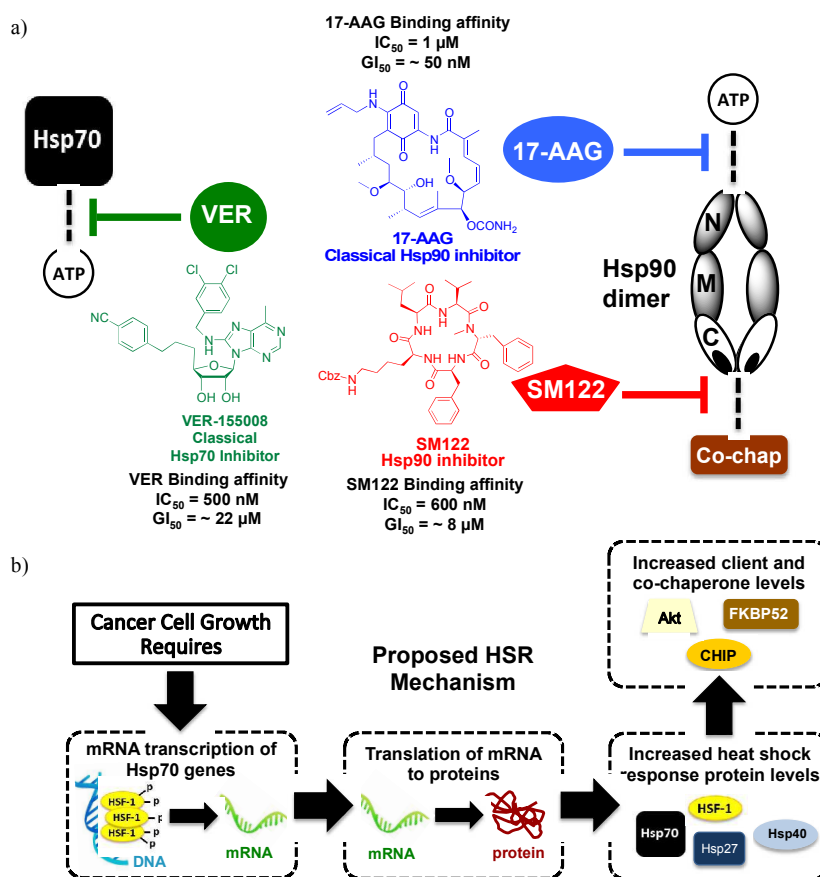


Fig. 1. a) The Hsp90 and Hsp70 inhibitors used in this study and where they impact their protein targets. b) The HSR mechanism that is activated during cancer growth. After treatment with the combination of VER/17-AAG or VER/SM122 each step of this mechanism is evaluated.

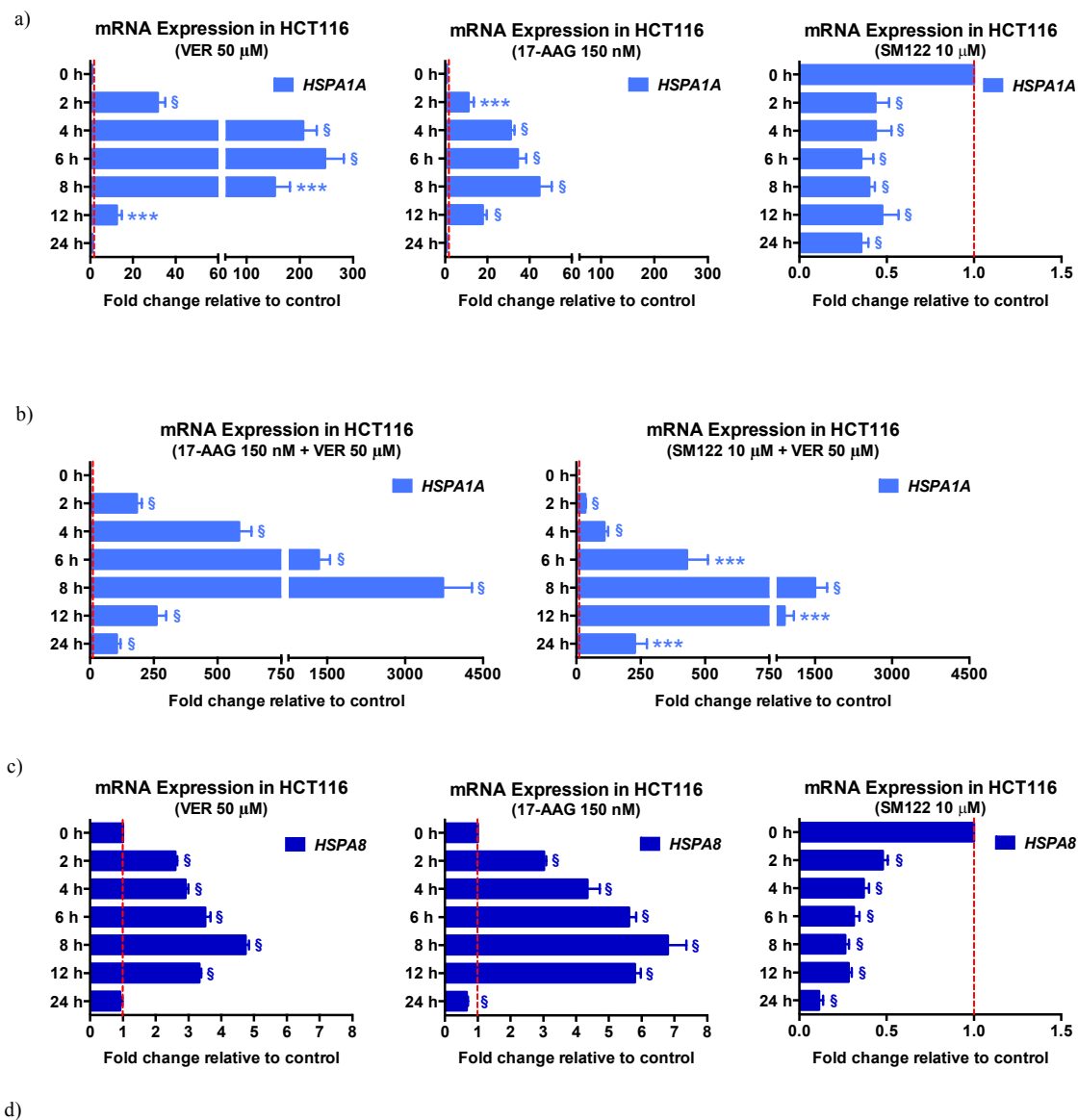
The combined impact of HSP dual inhibition on HSR induction was explored by evaluating the mRNA expression of HSPs. Since Hsp70 proteins are biomarkers of HSR induction, we studied two Hsp70 isoforms, the inducible Hsp72 (*HSPA1A*) and the constitutively expressed Hsc70 (*HSPA8*). In single-drug treatments against HCT116 cells, VER (50 μM) and 17-AAG (150 nM) dramatically up-regulated the mRNA expression levels of both hsp70 isoforms (Fig. 2a). Specifically, for the mRNA encoding *HSPA1A*, VER (50 μM) produced a maximum increase of ~ 250 fold over the control level (0 h time point) after 8 h-treatment, whereas 17-AAG (150 nM) induced up to ~ 45 fold over the control level at the same time point. Thus, it is clear that individually inhibiting Hsp70 or Hsp90 by targeting the ATP-binding site of HSPs strongly triggers the HSR at the transcription level. When treating HCT116 cells with a combination of 17-AAG and VER using the same concentrations elevated the mRNA expression level of *HSPA1A* by more than 3500 fold over the control level (Fig. 2b). Such an extreme increase caused by 17-AAG/VER-mediated combination treatment indicated that HCT116 cells experienced intense stress when Hsp90 and Hsp70 are simultaneously functionally suppressed.

In response to dual HSP inhibition, cancer cells rapidly initiate the HSR as a rescue mechanism: after only 2 hrs the mRNA expression level of *HSPA1A* has already reached ~ 200 fold of the control, whereas 17-AAG and VER alone caused a ~ 40 fold and ~ 15 fold increase, respectively, at the same time point (Fig. 2a and b). SM122 decreased the production of mRNA encoding for *HSPA1A*

by ~ 2 fold.¹⁵ Similar to 17-AAG/VER, treatment with SM122/VER also induced high levels of *HSPA1A* mRNA, peaking at ~ 1500 fold (Fig. 2b). In summary, 17-AAG/VER induces ~ 3500 fold increase in *HSPA1A* where as SM122/VER induces ~ 1500 fold, which suggests that SM122 suppresses the induction of *HSPA1A*. Moreover, SM122/VER did not trigger the HSR as rapidly as 17-AAG/VER did: the *HSPA1A* mRNA level was ~ 34 fold of the control after 2 hrs and ~ 108 fold after 4 hrs, whereas VER alone already caused ~ 30 and ~ 206 fold increase, respectively (Fig. 2a and b). Thus, SM122 appears to both suppress and delay the *HSPA1A* mRNA expression when used in combination with VER.

Evaluating *HSPA8* mRNA expression in treated HCT116 cells using 17-AAG and VER alone showed an increase in up to 5 and 7 fold over the control, respectively (Fig. 2c). Treating cells with the combination of 17-AAG/VER generated a maximum increase in mRNA expression of ~ 7 fold over control (Fig. 2d). Treating cells with SM122 alone decreased mRNA expression of *HSPA8* by ~ 10 fold (Fig. 2c), and using a combination of SM122/VER produces a maximum increase of 4 fold over control (Fig. 2d). Thus, SM122 still exhibits a suppressive effect although it is less obvious in transcription of *HSPA8* than with *HSPA1A*. These data support the hypothesis that although inhibiting both Hsp90 and Hsp70 function strongly induces a HSR rescue mechanism, the HSR can be moderated by using a C-terminal Hsp90 inhibitor.

COMMUNICATION



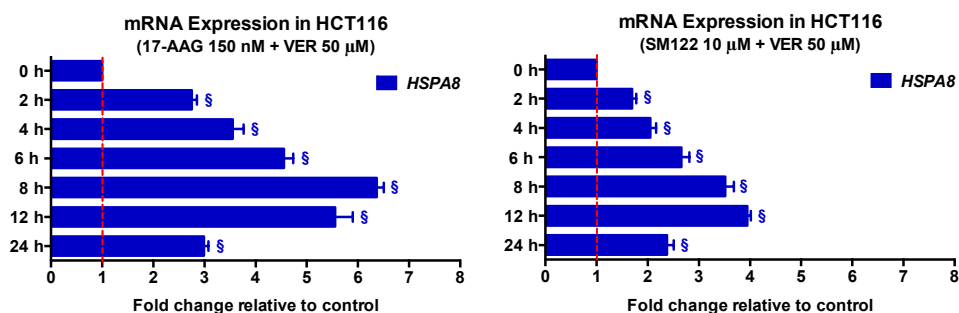


Fig. 2. mRNA expression levels of genes encoding for (a, b) heat-inducible Hsp72 (*HSPA1A*), and (c, d) constitutively expressed Hsc70 (*HSPA8*) over multiple time points in the HCT116 cells treated with VER, 17-AAG, SM122, 17-AAG/VER, or SM122/VER for 24 hrs. Data are average \pm s.e.m. from three independent experiments. Differences between treatments and indicated control treatment are represented with P values (*, $P < 0.05$; **, $P < 0.01$; ***, $P < 0.005$; and §, $P < 0.001$).

Evaluating the impact of inhibiting Hsp90 and Hsp70 on the translation process, involved performing a rabbit reticulocyte lysate (RRL)-based translation assay. In the RRL system the luciferase mRNA can be translated into luciferase proteins, and when correctly folded by the chaperones it generates a luminescent signal. The inhibitory effect of drug treatments on translation can be quantitatively indicated by the decrease of luminescence signal compared to the DMSO treatment (control). Incubation of the RRL with 5 μ M of 17-AAG at 37°C for 5 hrs resulted in an 8% decrease of luminescence (Fig. 3a). However, under the same treatment conditions, SM122 caused a 90% luminescence decrease in RRL (Fig. 3a). Similar to 17-AAG, VER has very little impact on translation (Fig. 3a). Thus, SM122 suppresses the mRNA translation process while both VER and 17-AAG cannot.

This translation assay produces the luminescence signal after two steps are completed in the lysate: a) translation of mRNA to unfolded protein and b) protein folding. Both steps require chaperones, where the first step of mRNA translation to unfolded protein requires the C-terminal end of Hsp90 to interact with the ribosome. Thus, blocking this interaction using a C-terminal modulator such as SM122 inhibits translation. The second step involves protein folding and is well established to be inhibited by 17-AAG, VER, and SM122. However, as our data shows, only SM122 inhibits the luminescence signal production, which is logical given that SM122 blocks ribosome access to Hsp90's C-terminus.

Combining 17-AAG (5 μ M) with VER (10 or 20 μ M) failed to significantly suppress the translation activity; in contrast, SM122 (1 μ M) combined with VER (10 or 20 μ M) showed a synergistic inhibitory effect (Fig. 3b). The most likely explanation for this observation is that SM122 blocked mRNA translation in the dual treatment (i.e. step 1 in the assay), while VER enhanced the inhibition of the protein folding process (i.e. step 2)¹⁶. These differences observed between treatments using 17-AAG versus SM122 supports our previous evidence that N-terminal and C-terminal modulators of Hsp90 have unique phenotypes.¹⁵

a) b)

Evaluating HSP induction showed that large increases of HSF-1, Hsp70, Hsp40, and Hsp27 protein levels were induced when treating HCT116 cells with the optimized doses of 17-AAG, VER, or 17-AAG/VER (Fig. 4a). As reported earlier, treatment with SM122 decreases these protein levels in HCT116 cells after 24 hrs.¹⁵ Dual treatment with the optimized doses of SM122/VER produced higher levels of HSPs than treating with SM122 alone, but protein levels remained equal to treatments with VER alone (Fig. 4b). Our data highlight how Hsp90 inhibitors that have different inhibitory mechanisms of action, i.e. 17-AAG versus SM122, will exhibit distinct phenotypes on the HSP induction in dual inhibition treatments. Specifically, we show that blocking the ATP-Hsp90 binding using 17-AAG increases the overall HSP accumulation when both chaperones are repressed. While utilizing a molecule that does not induce a HSR, e.g. SM122, moderates the HSP levels to the same fold change as those induced by VER alone. One interesting aspect is that Hsp27 decreased when cells were co-treated with VER and SM122 versus VER treatment alone (Fig. 4b). These data suggest that SM122 is able to moderate VER's impact specifically on Hsp27 levels during the HSR when using dual treatment.

In response to Hsp90 inhibition, a large number of co-chaperones and client proteins that interact with Hsp90 display decreased stability or increased degradation rates. Many of them contribute to pathways that promote tumour growth and survival. Since these proteins are highly dependent on Hsp90's chaperone roles in protein folding or stabilization, we examined their expression levels when functionally inhibiting both Hsp90 and Hsp70. Our hypothesis is that concurrently repressing a second major chaperone, Hsp70, would enhance the effect of Hsp90 inhibition on the depletion of these proteins. Synergistic degradation of these co-chaperones and clients could explain the observed synergistic effects in cytotoxicity, and inhibition of protein folding.¹⁶

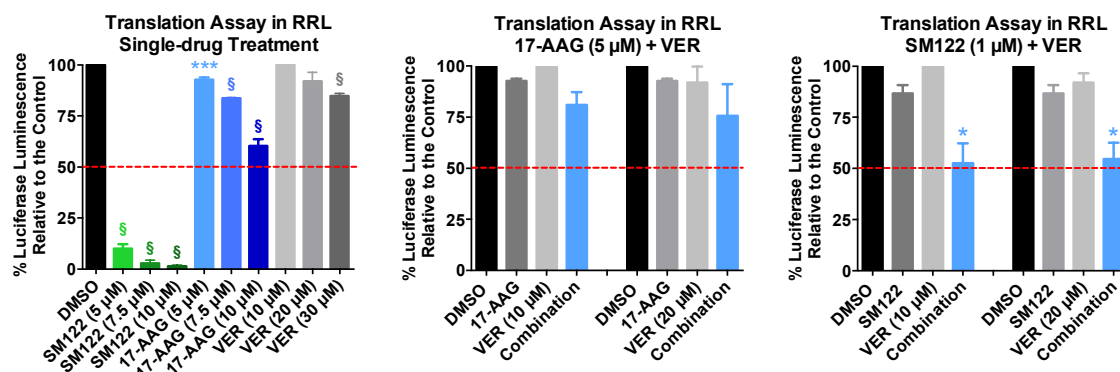


Fig. 3. Translation of luciferase mRNA to protein in the RRL translation system treated with (a) SM122, 17-AAG, or VER with indicated concentrations for 5 hrs, and (b) 17-AAG/VER or SM122/VER with indicated concentrations for 5 hrs. Data are average \pm s.e.m. from three independent experiments. Differences between treatments and DMSO control treatment are represented with P values (*, $P < 0.05$; **, $P < 0.01$; ***, $P < 0.005$; and §, $P < 0.001$).

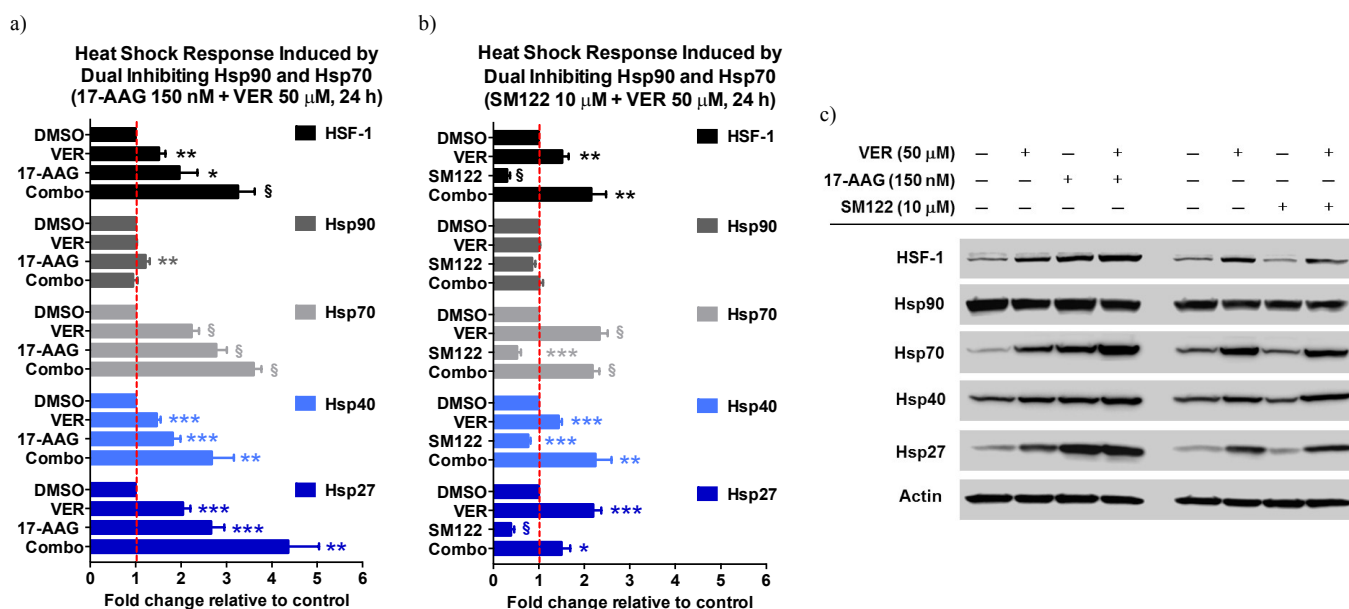


Fig. 4. Effect of HSP dual inhibition on HSF-1 and HSR induction. Immunoblot results are plotted as fold change relative to DMSO control when treating HCT116 cells with (a) 17-AAG, VER, or 17-AAG/VER, and (b) SM122, VER, or SM122/VER, with indicated concentrations for 24 hrs. All values are average \pm s.e.m. from three independent experiments. Differences between drug treatments and DMSO treatment (control) are represented with P values (*, $P < 0.05$; **, $P < 0.01$; ***, $P < 0.005$; and §, $P < 0.001$). (c) Immunoblot images. Actin was used as the protein loading control. All experiments were performed at least three times, and representative results are shown.

Immunophilins, including FKBP51, FKBP52, and their homologs such as CHIP, are well known for their ability to regulate cell growth through their interactions with Hsp90.²¹ Specifically, these immunophilins and homologs regulate the maturation of hormone receptors by forming a multi-chaperone complex with Hsp90, which induces a signaling cascade that leads to cancer cell growth.²¹ The down-regulation of numerous Hsp90 co-chaperones has been reported when using 17-AAG,²² however, 24 h-treatment of HCT116 cells with 17-AAG (100 ~ 1000 nM) had no impact on

FKBP52 or CHIP (Fig. 5a). Conversely, SM122 treatment resulted in a significant down-regulation of these two co-chaperones, highlighting the mechanistic difference between 17-AAG and SM122 (Fig. 5a). Interestingly, 17-AAG (150 nM) and VER (50 μ M) failed to affect these two co-chaperones individually, yet their combination effectively reduced FKBP52 by 36% and CHIP by 86% (Fig. 5b). Treating cells with SM122/VER also reduced protein levels of FKBP52 and CHIP (Fig. 5c), with a synergistic interaction seen on FKBP52.

Akt is a client of Hsp90 that plays a key role in multiple signaling pathways, and is constitutively activated in numerous cancer types in order to promote cellular survival and facilitate drug resistance.²³ Hsp90 stabilizes Akt by forming an Hsp90-Akt complex and facilitates its activation. Inhibiting Hsp90 results in Akt dephosphorylation *in vivo*, which leads to decreased Akt kinase activity and induced apoptosis. 24 h-treatment with 17-AAG (150 nM) decreased the total Akt in HCT116 cells by 36%, and 24 h-treatment with VER (50 μ M) reduced it by 45%. Remarkably, 17-AAG/VER co-treatment induced 95% degradation of Akt (Fig. 5c) at the same time point. Treating cells with SM122 (10 μ M) caused a 40% reduction of Akt. However, treatment with SM122/VER induced a 75% degradation of Akt (Fig. 5d). Thus, simultaneously

suppressing Hsp90 and Hsp70 can cause an abrupt and dramatic Akt depletion, which confirms the observed synergism in the cytotoxicity assays when using dual inhibitors.¹⁶ It appears that despite the increased HSP levels induced by 17-AAG/VER co-treatment, this combination results in dramatic co-chaperone degradation, which does not occur when either inhibitor is used individually. In contrast, treatment with a SM122/VER combination appears to rely primarily on SM122's ability to promote the co-chaperone degradation with a small synergistic effect between two inhibitors.

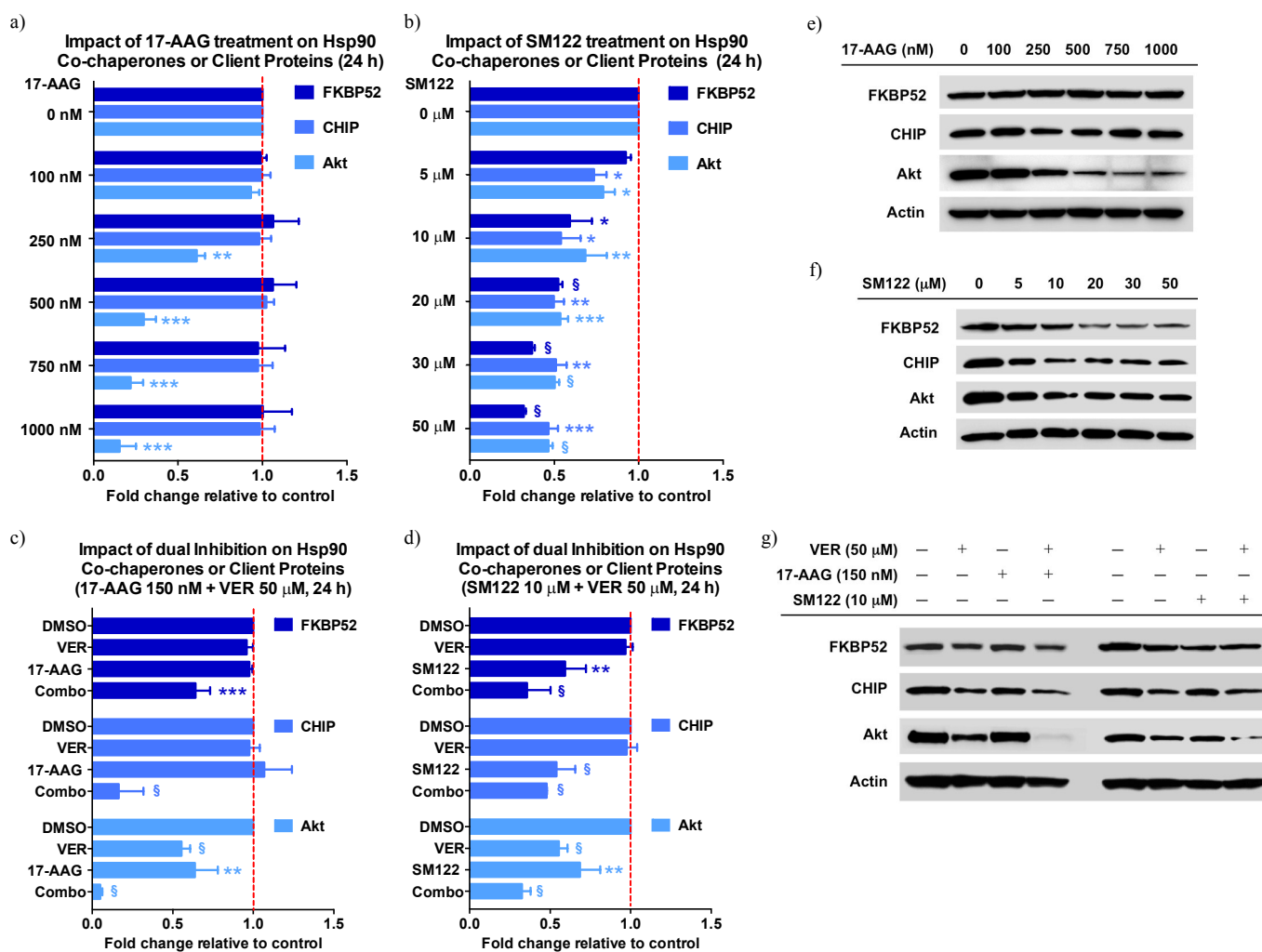


Fig. 5. Effects of HSP individual and dual inhibition on the protein expression of co-chaperones (FKBP52 and CHIP) and client protein (Akt). Immunoblot results are plotted as fold change relative to DMSO control when treating HCT116 cells with (a) 17-AAG, (b) SM122, (c) 17-AAG, VER, or 17-AAG/VER, and (d) SM122, VER, or SM122/VER, with indicated concentrations for 24 hrs. All values are average \pm s.e.m. from three independent experiments. Differences between drug treatments and DMSO treatment (control) are represented with *P* values (*, *P* < 0.05; **, *P* < 0.01; ***, *P* < 0.005; and §, *P* < 0.001). (e-g) Immunoblot images. Actin was used as the protein loading control. All experiments were performed at least three times, and representative results are shown.

COMMUNICATION

In summary, treatments with dual inhibitors 17-AAG/VER versus SM122/VER produce distinct mechanistic phenotypes. Assessing the impact of 17-AAG/VER on the mRNA expression levels of Hsp70s at transcription levels showed that Hsp90/Hsp70 dual inhibition induces higher cellular stress and triggers greater HSR as rescue mechanism than single HSP inhibition. SM122 modulates the overall impact of dual inhibition on mRNA production and reduces production levels compared to treatments with 17-AAG/VER. Furthermore, we demonstrate that SM122 has a significant suppression on translation both individually and in combination with VER, whereas 17-AAG/VER does not. This may explain our subsequent observation that the HSP protein expression levels in combination treatments are moderated by SM122, but are amplified when using 17-AAG. Finally, we see that HSP dual inhibition impacts the degradation of oncogenic proteins FKBP52, CHIP, and Akt, all of which exert cytoprotective or antiapoptotic roles in cancer cell survival. Thus, it is evident that alternative Hsp90 inhibitors can be utilized in dual cancer therapy regimens and produce similar results as the clinical drug 17-AAG. C-terminal modulators also have an advantage as they reduce the HSR, thereby potentially decreasing the levels of these cytoprotective proteins in cancer cells. Combination therapies using modulators such as SM122 may have high clinical impact.

Experimental

Cell lines and cell culture

HCT116 human colorectal carcinoma (CCL-247) cell line was obtained from ATCC (Manassas, Virginia, USA). Cells were cultured in Dulbecco's Modified Eagle Medium (DMEM) with supplements as proscribed by the manufacturer, and incubated in a humidified chamber at 37 °C with 5% CO₂.

Reagents, antibodies and primers

Stock solutions of 17-N-allylamino-17-demethoxygeldanamycin (17-AAG; Sigma Aldrich), SM122 (SRM laboratory), and VER-155008 (VER; Sigma Aldrich) were prepared by dissolving the solid compound in dimethyl sulfoxide (DMSO, Sigma Aldrich). Primary antibodies to HSF-1 (1 : 2,000), Hsp40 (1 : 2,000), and Hsp27 (1 : 2,000) were purchased from Abcam; Hsp90 (1 : 2,000), Hsp70 (1 : 2,000), and FKBP52 (1 : 2,000) were purchased from Enzo Life Sciences; CHIP (1 : 1,000) was purchased from Cell Signalling Technology; Akt (1 : 2,000) and Actin (1 : 4,000) was obtained from Santa Cruz Biotechnology. Secondary antibodies to goat anti-mouse HRP (1 : 2,000), goat anti-rabbit HRP (1 : 2,000), and rabbit anti-goat HRP (1 : 2,000) were obtained from Abcam. Primers for *HSPA8*, *HSPA1A*, and *18s* were purchased from Qiagen.

Quantitative real-time PCR assays

HCT116 cells were seeded into 6-well plates with a density of 5×10^5 cells per well 24 hrs before indicated treatments. Cells were exposed to drugs for a certain time period at 37 °C. Total RNA from each treatment (sample) was extracted using RNeasy Plus Mini Kit (Qiagen). cDNA was synthesized from prepared RNA samples using QuantiTect Reverse Transcription Kit (Qiagen). RT-PCR was performed in ViiA 7-Real Time PCR system (Life Technologies) using QuantiFast SYBR Green PCR Kit (Qiagen). Data were analyzed by using ViiA 7 Software. All experimental processes are performed following the manufacturer's instructions.

RRL-based translation assay

0.4 μL of DMSO (control) or single inhibitor, or 0.2 μL of each inhibitor in combination with indicated concentrations was incubated with 37.6 μL of 50% diluted rabbit reticulocyte lysate (RRL; Promega) in Mili-Q water at 30 °C for 5 hrs. 0.4 μL of amino acid mixture minus leucine, 0.4 μL of amino acid mixture minus methionine, and 0.4 μL of RNasin ribonuclease inhibitor were then added into the treated RRL translation system. The translation process was initiated by adding 0.8 μL of firefly luciferase mRNA (Promega) into the RRL and reactions were performed at 30 °C. After 60 min, 10 μL of each reaction mixture was removed and added to 40 μL of Bright-Glo™ luciferase assay buffer (Promega) mixed with Bright-Glo™ luciferase assay substrate (Promega), which was preloaded in a white, flat-bottomed, 96-well plate (Greiner Bio-One). After incubating for 2 min at room temperature in dark, the luminescence was measured using a luminometer (Berthold Orion Microplate Luminometer).

Immunoblotting

HCT116 cells were seeded in 6-well plates (5×10^5 cells per well) and incubated for 24 hrs before treatments. Cells were treated with indicated drugs for a certain time period and then lysed in lysis buffer (50 mM Tris-HCl, pH 7.4, 150 mM NaCl, 0.5% sodium deoxycholate and 0.5% NP40) supplemented with cocktail protease inhibitors (Roche). The total protein concentrations of lysates were determined by the bicinchoninic acid (BCA) method with the BCA kit (Pierce) following the manufacturer's instructions. 100 μg of total protein were separated by 4 ~ 20% Tris-Glycine gel (Life Technologies) and transferred to a PVDF membrane (Thermo Fisher Scientific). Membranes were blocked with 5% non-fat milk in TBST (Tris-buffered saline containing 0.1% Tween-20) for 2 hrs and incubated with respective primary antibodies in 2.5% non-fat milk (in TBST) at 4 °C overnight. After wash with cold TBST membranes were incubated with respective HRP-conjugated secondary antibodies at 4 °C for 2 hrs, following by three-time wash with cold TBST and one wash with cold TBS (Tris-buffered saline). Immunoblotting was performed using chemiluminescent substrates (Thermo scientific) and the images were captured by ImageQuant LAS 4010 digital imaging system (GE Healthcare). Data was quantified by ImageJ software.

Statistical analysis

To determine the statistical significance of experimental data, the unpaired Student *t* test was conducted using GraphPad Prism 6.0 (GraphPad Software Inc). Data were represented as mean \pm s.e.m. from at least three independent experiments. Differences are indicated with *P* values, which less than 0.05 were considered statistically significant relative to indicated comparison and designated with asterisk (*, *P* < 0.05; **, *P* < 0.01; ***, *P* < 0.005; and §, *P* < 0.001).

Notes and references

Department of chemistry, Gate 2 High street, Dalton 219, University of New South Wales, Sydney, NSW, 2052, Australia, email: s.mcalpine@unsw.edu.au

Electronic Supplementary Information (ESI) available: [details of all experimental methods, and raw data are included in the supplementary]. See DOI: 10.1039/c000000x/

1. J. E. Bohonowych, U. Gopal and J. S. Isaacs, *J. Oncol.*, 2010, 412-485.
2. L. Neckers, *J. Biosci.*, 2007, **32**, 517-530.
3. I. Fierro-Monti, Echeverria, P., Racle, J., Hernandez, C., Picard, D., Quadroni, M., *PLoS One*, 2013, **8**, e80425.
4. M. Taipale, Krykbaeva, I., Koeva, M., Kayatekin, C., Westover, K. D., Karras, G. I., Lindquist, S., *Cell*, 2012, **150**, 987-1001.
5. G. Chiosis, H. JHuezo, N. Rosen, E. Mimgaugh, L. Whitesell and L. Neckers, *Mol. Cancer Ther.*, 2003, **2**, 123-129.
6. D. Mahalingam, R. Swords, J. S. Carew, S. T. Nawrocki, K. Bhalla and F. J. Giles, *Br. J. Cancer*, 2009, **100**, 1523-1529.
7. M. Chatterjee, M. Andrulis, T. Stühmer, E. Müller, C. Hofmann, T. Steinbrunn, T. Heimberger, H. Schraud, S. Kressmann, H. Einsele and R. C. Bargou, *Haematologica*, 2013, **98**, 1132-1141.
8. H. Reikvam, I. Nepstad, A. Sulen, B. T. Gjertsen, K. J. Hatfield and Ø. Bruserud, *Expert Opin. Investig. Drugs.*, 2013, **22**, 551-563.
9. A. J. Massey, D. S. Williamson, H. Browne, et al., *Cancer Chemother. Pharmacol.*, 2010, **66**, 535-545.
10. E. L. Davenport, A. Zeisig, L. I. Aronson, H. E. Moore, S. Hockley, D. Gonzalez, E. M. Smith, M. V. Powers, S. Y. Sharp, P. Workman, G. J. Morgan and F. E. Davies, *Leukemia*, 2010, **24**, 1804-1807.
11. J. M. McConnell, L. D. Alexander and S. R. McAlpine, *Bioorg. Med. Chem. Lett.*, 2014, **24**, 661-666.
12. V. C. Ardi, L. D. Alexander, V. A. Johnson and S. R. McAlpine, *ACS Chem. Biol.*, 2011, **6**, 1357-1367.
13. Y. C. Koay, J. R. McConnell, Y. Wang, S. J. Kim and S. R. McAlpine, *ACS Med. Chem. Lett.*, 2014, **5**, 771-776.
14. J. D. Eskew, T. Sadikot, P. Morales, et al., *Bio. Med. Central Cancer.*, 2011, **11**, 468.
15. Y. Wang and S. R. McAlpine, *In press Chem. Comm.*, 2014, DOI: 10.1039/C1034CC07284G.
16. Y. Wang and S. R. McAlpine, *Submitted*, 2014.
17. J. B. Kunicki, M. N. Petersen, L. D. Alexander, V. C. Ardi, J. R. McConnell and S. R. McAlpine, *Bioorg. Med. Chem. Lett.*, 2011, **21**, 4716-4719.
18. L. D. Alexander, J. R. Partridge, D. A. Agard and S. R. McAlpine, *Bioorg. Med. Chem. Lett.*, 2011, **21**, 7068-7071.
19. R. C. Vasko, R. A. Rodriguez, C. N. Cunningham, V. C. Ardi, D. A. Agard and S. R. McAlpine, *ACS Med. Chem. Lett.*, 2010, **1**, 4-8.
20. R. P. Sellers, L. D. Alexander, V. A. Johnson, et al., *Bioorg. Med. Chem.*, 2010, **18**, 6822-6856.
21. P. Echeverria and D. Picard, *Biochim. Biophys. Acta.*, 2010, **1803**, 641-649.
22. L. Whitesell, S. Santagata and N. U. Lin, *Curr. Mol. Med.*, 2012, **12**, 1108-1124.
23. J. G. LoPiccolo, C. A.; Gills, J. J.; Dennis, P. A., *Anticancer Drugs*, 2007, **18**, 861-874.

